High-Resolution Molecular Orbital Imaging Using a *p*-Wave STM Tip

Leo Gross,[1,*] Nikolaj Moll,[1] Fabian Mohn,[1] Alessandro Curioni,[1] Gerhard Meyer,[1] Felix Hanke,[2] and Mats Persson[2]

[1]*IBM Research—Zurich, 8803 Rüschlikon, Switzerland*
[2]*Surface Science Research Centre, Department of Chemistry, University of Liverpool, Liverpool, L69 3BX, United Kingdom*

Individual pentacene and naphthalocyanine molecules adsorbed on a bilayer of NaCl grown on Cu(111) were investigated by means of scanning tunneling microscopy using CO-functionalized tips. The images of the frontier molecular orbitals show an increased lateral resolution compared with those of the bare tip and reflect the modulus squared of the lateral gradient of the wave functions. The contrast is explained by tunneling through the *p*-wave orbitals of the CO molecule. Comparison with calculations using a Tersoff-Hamann approach, including *s*- and *p*-wave tip states, demonstrates the significant contribution of *p*-wave tip states.

PACS numbers: 68.37.Ef, 71.15.Mb, 73.20.Hb, 73.61.Ng

The role of the tip wave function in scanning tunneling microscopy (STM) has been discussed in great detail in several theoretical studies and is of fundamental importance for the interpretation of STM images [1,2]. It was shown early on by Tersoff and Hamann [1] that for *s*-wave tip states, STM images approximately resemble the local density of states, which is given by the modulus squared of sample wave functions evaluated at the Fermi energy. In contrast, for *p*-wave tip states, STM images are expected to show spatial derivatives of the sample wave functions, as pointed out by Chen in his derivative rule [2–4].

The character of tip states could in principle be modified by functionalizing the tip by picking up single atoms and molecules. Several groups have shown that a tip termination using either metal atoms, CO, H_2 or organic molecules leads to an enhanced resolution of STM images compared to the bare tip [5–16]. In particular, the lobes of frontier molecular orbitals of planar organic molecules could be resolved with increased resolution using pentacene-terminated tips [9–11]. In the latter case the increased resolution is explained by a decrease of the effective tip-sample distance compared with bare tips [9]. CO-terminated tips could give rise to tunneling through the $2\pi^*$ orbitals of CO and exhibit *p*-wave character [17]. However, to date no *p*-wave contributions have been identified in any images recorded using CO tips or any other functionalized tips.

By imaging molecular orbitals with a CO-functionalized tip at 5 K, we demonstrate in this Letter that the STM images represent the lateral gradient of the wave function, in agreement with Chen's derivative rule. A comparison with theory corroborates the significant contribution of *p*-wave tip states. A key finding with wide ramifications for the imaging of individual molecules is the observation that orbitals with closely spaced nodal planes can be imaged with high contrast because of a large lateral gradient of the wave function.

As model systems we investigated pentacene and naphthalocyanine. For each model system, the structure, highest

occupied molecular orbital (HOMO), and lowest unoccupied molecular orbital (LUMO) are shown schematically in Fig. 1. To decouple the molecules electronically from the substrate and to suppress direct tunneling into the metal substrate, we used a two-monolayer (ML) thick NaCl film deposited on Cu(111). As shown by Repp *et al.* [9], two distinct molecular resonances are observable for pentacene on NaCl(2 ML)/Cu(111) in the dI/dV spectra, centered at $V = -2.4$ V and at $V = 1.7$ V, corresponding to the positive ion resonance (PIR) and negative ion resonance (NIR), respectively. At these voltages, electrons predominantly tunnel through the HOMO and through the LUMO, respectively, and STM images acquired at these voltages resemble the shape of their orbital densities when using *s*-wave tips [9]. We created a Cu tip, i.e., an *s*-wave tip, by bringing a PtIr tip, cut by focused ion beam, into controlled contact with the Cu(111) surface. Finally, to create a CO tip, a single CO molecule was picked up as described previously [5,18]. Compared with images obtained with *s*-wave tips, the orbital images change drastically when using a CO tip as shown in Figs. 2(a) and 2(b).

Calculated constant-height images of the HOMO and LUMO using the Tersoff-Hamann [1] approach with an
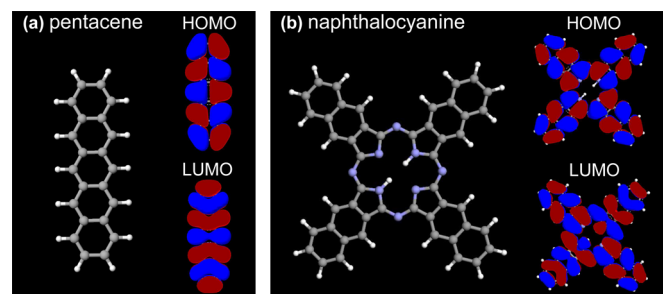

FIG. 1 (color online). Structure model and molecular frontier orbitals HOMO and LUMO of (a) pentacene and (b) naphthalocyanine. The colors of the atoms correspond to carbon (gray), hydrogen (white) and nitrogen (blue [medium-light gray]). Images were calculated with ArgusLab [31].

s-wave tip are shown in Figs. 2(c) and 2(d), respectively. They correspond to STM measurements with metal- or pentacene-terminated tips [9]. The calculated images for the *s*-wave tip were obtained from the orbital density $A_s(x, y) = |\Psi(x, y, z_0)|^2$, where $\Psi(x, y, z_0)$ is the HOMO or LUMO of the isolated pentacene molecule, respectively, at a fixed distance z_0 to the molecular plane. By convention, *x* and *y* denote the axes within the molecular plane, whereas the *z* axis is orthogonal to it. The HOMO and LUMO were calculated by employing density functional theory [19] and the highly optimized CPMD code [20]. We applied the Perdew-Burke-Ernzerhof exchange-correlation functional [21] and *ab initio* norm-conserving pseudopotentials [22]. The wave functions were expanded into plane waves [23] with a kinetic energy of up to 300 Ry. In accordance with Chen's derivative rule [2], the elements of the tunneling matrix *M* for a tip exhibiting a p_x and a p_y tip state (corresponding to the two degenerate $2\pi^*$ orbitals of the CO) become

$$M_{p_x} \propto \frac{\partial \Psi}{\partial x} \quad \text{and} \quad M_{p_y} \propto \frac{\partial \Psi}{\partial y}, \qquad (1)$$

respectively. As the tunneling current is proportional to the sum of the squared tunneling matrix elements, we calculated the images for the *p*-wave tip from the modulus squared of the lateral gradient of the orbitals as

$$A_p(x, y) = \left| \frac{\partial \Psi(x, y, z_0)}{\partial x} \right|^2 + \left| \frac{\partial \Psi(x, y, z_0)}{\partial y} \right|^2. \qquad (2)$$

Figures 2(e) and 2(f) show the calculated constant-height images of the HOMO and LUMO of pentacene when

using a *p*-wave tip. They exhibit an overall good qualitative agreement with the experimental images in Figs. 2(a) and 2(b). For example, in contrast to the *s*-wave tip images, the number and location of nodal planes are correctly reproduced. From this observation we infer that a significant part of the electron tunneling occurs through the degenerate π_x and π_y orbitals of the CO molecule, which exhibit *p*-wave character with respect to the O atom and have the nodal planes orthogonal to the sample surface [24].

To obtain a more intuitive explanation for the observed contrast, we have examined three high-symmetry tip positions as shown schematically in Fig. 3. In the first case shown in Fig. 3(a), the tip is located above the center in a lobe of the pentacene orbital. The pentacene orbital locally exhibits σ character (in the bottom panel of Fig. 3 a dotted circle is drawn as a guide to the eye). Contributions from positive and negative lobes of the *p*-wave tip orbital to the tunneling amplitude cancel each other out effectively, as illustrated in the side view in Fig. 3(a), so that $M = 0$. More generally, if the sample wave function is locally point symmetric in the *xy* plane around the tip position, a minimum is expected in the contrast. With this argument, we can understand the minima measured at the position of the orbital lobes.

In the second high-symmetry position, shown in Fig. 3(b), the tip is located above a single nodal plane of the molecular orbital; hence, the sample wave function locally exhibits π character. In this case, contributions to the tunneling amplitude from the two lobes of the p_x orbital of the tip have the same sign, because the phase (sign) change in the p_x orbital of the tip is accompanied by
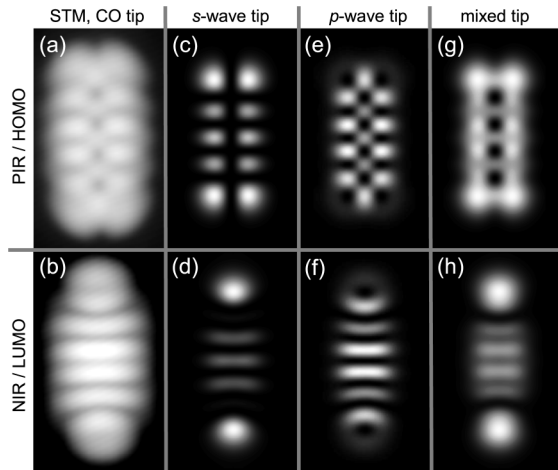

FIG. 2. STM measurements of pentacene on NaCl(2 ML) on Cu(111) using a CO tip at the onset (a) of the PIR at $V = -2.15$ V, $I = 0.9$ pA, and (b) of the NIR at $V = +1.25$ V, $I = 1.3$ pA. Calculated STM images at $z_0 = 4.5$ Å of the HOMO and LUMO of the isolated molecule, respectively, using the Tersoff-Hamann approach with an *s*-wave tip (c),(d), a *p*-wave tip (e),(f), and an *sp*-wave mixed tip (g),(h). All images: 15 Å × 25 Å.
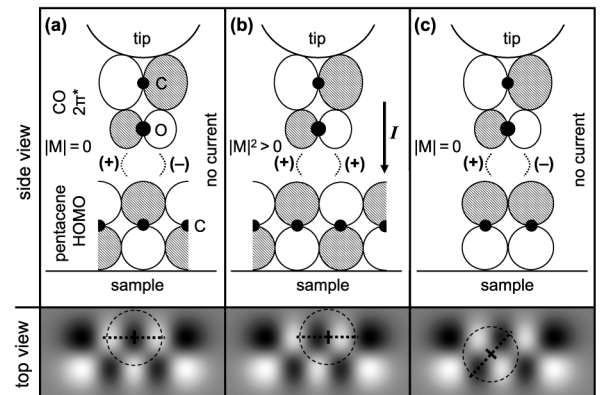

FIG. 3. Schematic of tunneling between the CO $2\pi^*$ orbital (tip) and pentacene HOMO (sample) for different positions. The bottom panels show top views of the pentacene HOMO, with dotted lines indicating the positions and orientations of the cut planes shown in the schematics above. Different gray scales correspond to different signs of the wave function. Locally the pentacene orbital exhibits σ (a), π (b), and δ (c) character, respectively. Because of the *p*-wave character of the CO tip state, the tunneling matrix *M* and the tunneling current *I* become zero in (a) and (c), but not in (b).

a phase change also in the sample wave function, as shown schematically in Fig. 3(b). With this argument, we can understand the local maxima measured at the position of the orbital nodal planes [Fig. 2(b)].

In Fig. 3(c), we examine the tip position above the crossing of two nodal planes. In this case, the orbital locally exhibits δ character and opposing orbital lobes show no phase change. The phase change in the tip $p_{x,y}$ waves across these lobes then gives rise to vanishing tunneling matrix elements and currents. With this third argument we can now understand the contrast of the HOMO [Fig. 2(a)] showing depressions at the crossings of nodal planes. It is interesting to note that a d_{xy} tip state would lead to a maximum in this case and to minima in both the previous cases.

Differences between experimental images using a CO tip [Figs. 2(a) and 2(b)] and calculated images using a p-wave tip [Figs. 2(e) and 2(f)] mainly show up above the ends of the molecule, at the positions of the outer lobes of the LUMO and HOMO, where only the calculations exhibit local minima. Contributions from other tip states, for example, from the p_z-wave character 5σ orbital of CO, cannot be ruled out [17] and can enhance tunneling at the ends of the molecule. Note that a p_z-wave tip, due to the absence of nodal planes perpendicular to the surface, will generate contrast that is qualitatively similar to that of an s-wave tip [25]. We have taken s-wave tip contributions into account by calculating images from a simple superposition of the s-wave and p-wave tips defined by a mixed-tip amplitude

$$A_{\mathrm{mix}}(x, y) = \frac{A_s(x, y) + A_p(x, y)}{2}. \quad (3)$$

The resulting images are displayed in Figs. 2(g) and 2(h). For this mixed sp-wave tip, we obtain good qualitative agreement with the experiment, reproducing, in particular, the observed behavior at the ends of the molecule.

Note that for the pentacene molecule, the nodal planes can be resolved using an s-wave tip and that a p-wave tip gives no additional information. However, in the case of a naphthalocyanine molecule adsorbed on the same substrate, the nodal planes are closely spaced and are challenging to resolve using an s-wave tip [11] [Fig. 4(a)]. A p-wave tip, such as the CO tip, enhances the contrast and reveals additional information about the orbital structure also in the central region, as demonstrated in both the constant-current [Fig. 4(b)] and the constant-height images [Fig. 4(c)].

Calculated images for an s-wave tip [Fig. 4(d)] show qualitative agreement with the experimental data using a Cu tip [Fig. 4(a)], whereas the images calculated for a p-wave tip [Fig. 4(e)] show only partial agreement with images observed using a CO tip [Fig. 4(b)]. For a more direct comparison with our calculations, we measured STM images in constant-height mode [Fig. 4(c)] using a
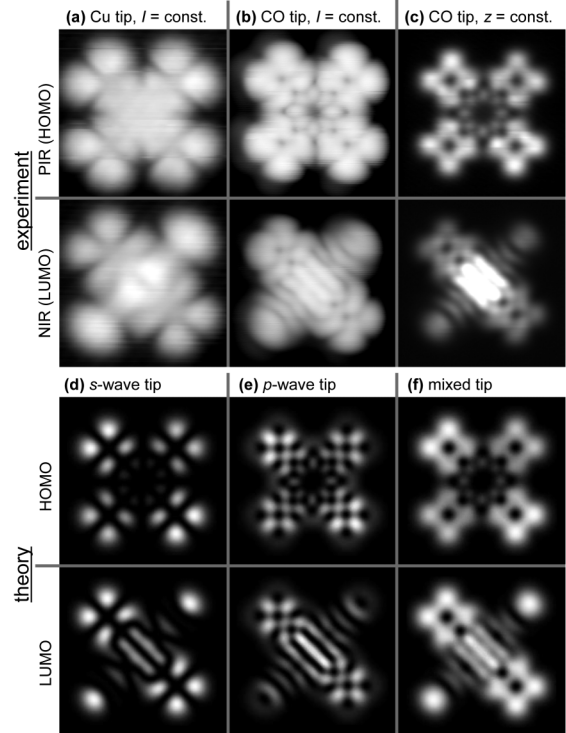

FIG. 4. Naphthalocyanine on NaCl(2 ML) on Cu(111) measured using a Cu tip (a) and a CO tip (b) in constant-current mode, and with a CO tip in constant-height mode (c). The PIR (1st row) is measured at $V = -1.65$ V and the NIR (2nd row) at $V = 0.60$ V. Calculated images at $z_0 = 5.0$ Å of the HOMO (3rd row) and LUMO (4th row) with an s-wave tip (d), a p-wave tip (e), and with a mixed tip (f). The molecule is oriented as depicted in Fig. 1(b). All images: 27 Å × 27 Å.

CO tip. Similarly to pentacene, we observe differences between experimental CO-tip images [Figs. 4(b) and 4(c)] and calculated p-wave tip images [Fig. 4(e)] above the outer lobes of the molecular orbitals, where we see local minima only in the calculations. Again we calculated images for the mixed tip with Eq. (3), reproduced in Fig. 4(f), which show excellent agreement with the constant-height images measured with a CO tip [Fig. 4(c)].

By comparing the calculated s-wave and p-wave tip images with the mixed-tip images, we find that the relative contributions of s- and p-wave character not only depend on the tip but also on the lateral tip position. On the one hand, the relative p-wave contribution of a CO tip is increased in regions where the lateral gradient of the orbital becomes large, e.g., in the central part of the molecule showing closely spaced nodal planes. On the other hand, the influence of the s-wave tip is enhanced at outspread maxima of the orbital, where the amplitude is large but the gradient is small, e.g., above the outermost lobes of the orbitals. For this reason, we abstain from any quantification of the s- and p-wave contributions. However, from the excellent agreement of the images calculated for the mixed tip with the experimental data, we can conclude that

p-wave tip states contribute significantly to the contrast measured, and that the contributions from *s*-wave tip states explain, for the most part, the deviations from a purely *p*-wave tip. For future investigations it might be interesting to compare *s*- and *p*-wave contributions of different tips, e.g., by using other tip terminations than CO or tips with different metal atoms behind the CO molecule.

There are several reasons why the direct observation of image contrast related to the lateral gradient of the sample wave function has so far only been achieved by measuring molecular orbitals on a thin insulating film. Most importantly, by resonant tunneling through a double barrier, the entire current passes through the adsorbate located between the barriers. Therefore interference effects with other tunneling channels, e.g., direct tunneling between tip and metal substrate [26], can be excluded. Moreover, molecular orbitals are well suited to reveal the *p*-wave character of the CO tip because both the sample and tip wave function show similar lateral sizes of the orbital lobes, and a large contrast is generated because of the overlap between tip and sample orbitals.

It is interesting to note that the contrast obtained by *p*-wave tips crucially depends on the relative phase of the sample wave function. For example, the maxima that result when the tip is positioned above a nodal plane reflect the phase (sign) change of the orbital [see Fig. 3(b)]. In contrast to the absolute value of the amplitude of a wave function, its phase is not directly observable; however, the relative phase is of great importance for bonding and conductivity. In a few examples, the phase of molecular orbitals could be mapped [27]. By using symmetry arguments, phase information could be added to photoemission data of molecules [28] or STM measurements for the case of Shockley surface state waves inside resonators [29]. As *p*-wave tips are sensitive to the relative phase, they might be useful to distinguish between bonding and antibonding combinations of orbitals [30] in the case of weak coupling.

In conclusion, we have demonstrated that STM orbital images obtained with a CO-functionalized tip show significant *p*-wave tip contributions due to tunneling through the π orbitals of the CO tip. The contrast reflects the lateral gradient of the wave function, in agreement with Chen's derivative rule [2]. Excellent agreement is obtained with respect to calculations using a Tersoff-Hamann approach with a mixed *sp*-wave tip. Because images obtained by *p*-wave tips achieve increased resolution and, moreover, rely crucially on the wave function phase, this method could be important in the further study of molecular switches [11] and metal-molecule complexes [10,15] whose functionality could be based on engineering of molecular orbitals.

*lgr@zurich.ibm.com

[1] J. Tersoff and D. R. Hamann, Phys. Rev. B **31**, 805 (1985).
[2] C. J. Chen, *Introduction to Scanning Tunneling Microscopy* (Oxford University Press, New York, 1993).
[3] C. J. Chen, J. Vac. Sci. Technol. A **6**, 319 (1988).
[4] C. J. Chen, Phys. Rev. B **42**, 8841 (1990).
[5] L. Bartels, G. Meyer, and K.-H. Rieder, Appl. Phys. Lett. **71**, 213 (1997).
[6] H. J. Lee and W. Ho, Science **286**, 1719 (1999).
[7] J. Lagoute, K. Kanisawa, and S. Fölsch, Phys. Rev. B **70**, 245415 (2004).
[8] T. Nishino, T. Ito, and Y. Umezawa, Proc. Natl. Acad. Sci. U.S.A. **102**, 5659 (2005).
[9] J. Repp, G. Meyer, S. M. Stojkovic, A. Gourdon, and C. Joachim, Phys. Rev. Lett. **94**, 026803 (2005).
[10] J. Repp, G. Meyer, S. Paavilainen, F. E. Olsson, and M. Persson, Science **312**, 1196 (2006).
[11] P. Liljeroth, J. Repp, and G. Meyer, Science **317**, 1203 (2007).
[12] Q.-M. Xu, L.-J. Wan, S.-X. Yin, C. Wang, and C.-L. Bai, J. Phys. Chem. B **105**, 10 465 (2001).
[13] R. Temirov, S. Soubatch, O. Neucheva, A. C. Lassise, and F. S. Tautz, New J. Phys. **10**, 053012 (2008).
[14] G. Schull, T. Frederiksen, M. Brandbyge, and R. Berndt, Phys. Rev. Lett. **103**, 206803 (2009).
[15] F. Mohn, J. Repp, L. Gross, G. Meyer, M. S. Dyer, and M. Persson, Phys. Rev. Lett. **105**, 266102 (2010).
[16] Z. Cheng *et al.*, Nano Res. **4**, 523 (2011).
[17] M. Paulsson, T. Frederiksen, H. Ueba, N. Lorente, and M. Brandbyge, Phys. Rev. Lett. **100**, 226604 (2008).
[18] L. Gross, F. Mohn, N. Moll, P. Liljeroth, and G. Meyer, Science **325**, 1110 (2009).
[19] P. Hohenberg and W. Kohn, Phys. Rev. **136**, B864 (1964).
[20] CPMD, Copyright IBM Corp. 19902010, Copyright MPI fur Festkorperforschung Stuttgart 19972001. http://www.cpmd.org.
[21] J. P. Perdew, K. Burke, and M. Ernzerhof, Phys. Rev. Lett. **77**, 3865 (1996).
[22] D. R. Hamann, Phys. Rev. B **40**, 2980 (1989).
[23] J. Ihm, A. Zunger, and M. L. Cohen, J. Phys. C **12**, 4409 (1979).
[24] Note that both the 1π and the $2\pi^*$ orbitals of CO exhibit the same axial symmetry with respect to the surface plane. Therefore, tunneling through the 1π orbitals cannot be ruled out considering our experimental results.
[25] F. E. Olsson, N. Lorente, and M. Persson, Surf. Sci. **522**, L27 (2003).
[26] J. A. Nieminen, E. Niemi, and K.-H. Rieder, Surf. Sci. **552**, L47 (2004).
[27] J. Itatani *et al.*, Nature (London) **432**, 867 (2004).
[28] P. Puschnig *et al.*, Science **326**, 702 (2009).
[29] C. R. Moon, L. S. Mattos, B. K. Foster, G. Zeltzer, W. Ko, and H. C. Manoharan, Science **319**, 782 (2008).
[30] A. Shiotari, Y. Kitaguchi, H. Okuyama, S. Hatta, and T. Aruga, Phys. Rev. Lett. **106**, 156104 (2011).
[31] ArgusLab 4.0.1, M. A. Thompson, Planaria Software LLC, Seattle, WA, http://www.arguslab.com.